ISSN 1064-2269, Journal of Communications Technology and Electronics, 2014, Vol. 59, No. 6, pp. 523–535. © Pleiades Publishing, Inc., 2014.
Original Russian Text © V.S. Vlasov, V.G. Shavrov, V.I. Shcheglov, 2014, published in Radiotekhnika i Elektronika, 2014, Vol. 59, No. 6, pp. 572–586.

RADIO PHENOMENA IN SOLIDS AND PLASMA

Excitation of Hypersonic Oscillations under Magnetic Switching of a Normally Magnetized Ferrite Plate

V. S. Vlasov[a], V. G. Shavrov[b], and V. I. Shcheglov[b]

[a] *Syktyvkar State University, Oktyabr'skii pr. 55, Syktyvkar, 167001 Komi Republic, Russia*
[b] *Kotel'nikov Institute of Radio Engineering and Electronics, Russian Academy of Sciences, Mokhovaya ul. 11, korp. 7, Moscow, 125009 Russia*
e-mail: shelemba@iae.nsk.ru

Received July 3, 2013

Abstract—Hypersonic elastic oscillations are excited in the microwave range using magnetization reversal of a normally magnetized ferrite plate due to precession of the magnetization vector around the field direction. Characteristic times are determined for magnetic and elastic oscillations, and the relation of these times with decay parameters of both processes are demonstrated. An empirical analysis using exponential functions and a model of the quasi-static rotation of the magnetization vector are employed for interpretation of the effects. Prospects for application of the effects for the excitation of high-power microwave hypersound are discussed, and a possibility of elastic oscillations with amplitudes of up to 10^{-9} cm is demonstrated.

DOI: 10.1134/S1064226914050106

INTRODUCTION

There has been considerable recent interest in the excitation of ultrasonic oscillations using magnetostrictive transducers [1–4]. In conventional applications (hydroacoustics, defectoscopy, and ultrasonic technology), such transducers are used for excitation of low-frequency (up to hundreds of kilohertz) elastic oscillations. Note interest in the excitation of hypersonic oscillations at frequencies of up to tens of gigahertz, which makes it possible to develop high-efficiency devices for data processing in the microwave range ($f \sim 10^9$–10^{11} Hz). Yttrium-iron garnet (YIG) is a promising material, since the Q factor of the corresponding acoustic resonators amounts to 10^7.

Experimental results on the excitation of hypersound with the aid of the YIG magnetoacoustic transducers [4–7] yield relatively high efficiencies and relatively low decay of ultrasonic pulses: series of more than 100 rereflected pulses were observed at a frequency of 500 MHz (the number of pulses is significantly greater than that for quartz) [4]. However, such results can be achieved only at an input signal power of no greater than 1 mW [4, 7]. At higher powers, the loss substantially increases due to parametric decay of uniform precession into exchange spin waves [8–11].

In accordance with the results of [12–14], the parametric decay can be suppressed using an appropriate configuration of the transducer. In the optimal configuration, the lower frequency of the ferromagnetic resonance (FMR) of a normally magnetized thin disk coincides with the bottom of the spectrum of exchange spin waves, so that the parametric excitation of such waves and the corresponding loss vanish. The analysis of such a configuration in [15] shows that the amplitude of the excited hypersound can be increased by more than two orders of magnitude.

In the above works, the oscillations of magnetization are excited at a relatively high power of the microwave oscillator. Efficient excitation of magnetic oscillations at the FMR frequency is possible in the absence of such an oscillator due to magnetization reversal of a spherical ferrite sample in the presence of a stepwise field, which makes it possible to generate high-power microwave pulses. However, the working regime of such an oscillator can presumably be disturbed due to parametric excitation of exchange spin waves that may lead to an avalanche-type increase in the temperature of the sample and, hence, its destruction. Note that the suppression of exchange waves using appropriate configuration of the sample has not been considered. The analysis of excitation of elastic oscillations under such conditions due to magnetoelastic properties of ferrite is also missing.

In this work, we study the excitation of high-power microwave hypersound under pulsed magnetization reversal of ferrite in the configuration with a normally magnetized disk.

1. CONFIGURATION UNDER STUDY AND BASIC EQUATIONS

Figure 1 illustrates the configuration of the problem that coincides with that of [15]. A plane-parallel plate with thickness d exhibits magnetic, elastic, and magnetoelastic properties. External static magnetic

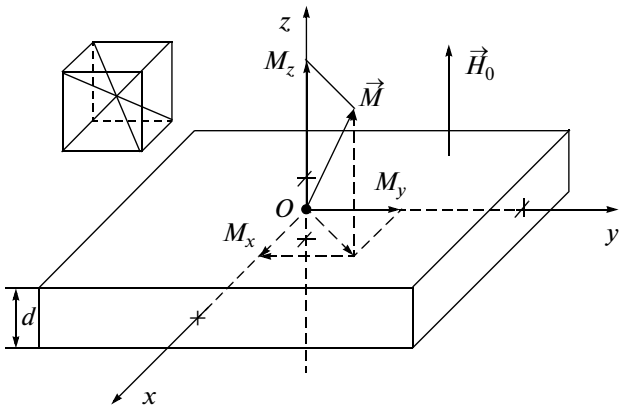

Fig. 1. Configuration of the problem.

field $\vec{H}_0$ is exerted orthogonally to the plate plane. We solve the problem using the Cartesian coordinates $Oxyz$: the Oxy plane coincides with the plate plane and the Ox, Oy, and Oz axes are parallel to the edges of the cube of crystallographic cell. Origin of coordinates is located at the center of the plate, so that $z = \pm d/2$ are coordinates of the plate planes. Figure 1 shows magnetization vector $\vec{M}$ and orientations of the axes of the cubic crystallographic cell.

We assume that total energy density U of the plate in the presence of the field $\vec{H} = \{0;0;H_0\}$ is equal to a sum of the magnetic, elastic, and magnetoelastic energy densities [15]. Thus, we obtain the following expression that contains significant terms:

$$U = -M_0 H_0 m_z + 2\pi M_0^2 m_z^2 + 2c_{44}\left(u_{xy}^2 + u_{yz}^2 + u_{zx}^2\right) + 2B_2(m_x m_y u_{xy} + m_y m_z u_{yz} + m_z m_x u_{zx}). \quad (1)$$

Here, $\vec{m} = \vec{M}/M_0$ is normalized magnetization vector, M_0 is saturation magnetization, c_{44} is elasticity constant (modulus), and B_2 is the constant of magnetoelastic interaction.

Using the approach from [15], we derive the system of equations and boundary conditions that contains

(i) equations for magnetization

$$\frac{\partial m_x}{\partial t} = -\frac{\gamma}{1+\alpha^2}\left[\left(m_y + \alpha m_x m_z\right)H_z - \left(m_z - \alpha m_y m_x\right)H_y - \alpha\left(m_y^2 + m_z^2\right)H_x\right]; \quad (2)$$

$$\frac{\partial m_y}{\partial t} = -\frac{\gamma}{1+\alpha^2}\left[\left(m_z + \alpha m_y m_x\right)H_x - \left(m_x - \alpha m_z m_y\right)H_z - \alpha\left(m_z^2 + m_x^2\right)H_y\right]; \quad (3)$$

$$\frac{\partial m_z}{\partial t} = -\frac{\gamma}{1+\alpha^2}\left[\left(m_x + \alpha m_z m_y\right)H_y - \left(m_y - \alpha m_x m_z\right)H_x - \alpha\left(m_x^2 + m_y^2\right)H_z\right]; \quad (4)$$

where effective fields are represented as

$$H_x = -\frac{B_2}{M_0} m_z \frac{\partial u_x}{\partial z}; \quad (5)$$

$$H_y = -\frac{B_2}{M_0} m_z \frac{\partial u_y}{\partial z}; \quad (6)$$

$$H_z = H_0 - 4\pi M_0 m_z - \frac{B_2}{M_0}\left(m_x \frac{\partial u_x}{\partial z} + m_y \frac{\partial u_y}{\partial z}\right); \quad (7)$$

(ii) equations for elastic displacement

$$\frac{\partial^2 u_x}{\partial t^2} = -2\beta\frac{\partial u_x}{\partial t} + \frac{c_{44}}{\rho}\frac{\partial^2 u_x}{\partial z^2}; \quad (8)$$

$$\frac{\partial^2 u_y}{\partial t^2} = -2\beta\frac{\partial u_y}{\partial t} + \frac{c_{44}}{\rho}\frac{\partial^2 u_y}{\partial z^2}; \quad (9)$$

and boundary conditions

$$c_{44}\frac{\partial u_x}{\partial z}\bigg|_{z=\pm d/2} = -B_2 m_x m_z; \quad (10)$$

$$c_{44}\frac{\partial u_y}{\partial z}\bigg|_{z=\pm d/2} = -B_2 m_y m_z. \quad (11)$$

Here, γ is gyromagnetic constant ($\gamma > 0$), α is decay parameter of magnetization, ρ is density of plate material, and β is decay parameter of elastic displacement.

The system of equations is used to solve the problem under study. The solution and transformations that are needed for numerical analysis can be found in [15]. Below, we present the results.

2. GENERAL SCENARIO OF THE EXCITATION OF HYPERSOUND UNDER MAGNETIZATION REVERSAL

In the initial state, static field H_0 that is higher than the demagnetization field ($H_0 > 4\pi M_0$, where M_0 is saturation magnetization of the magnetic plate) is oriented along the negative direction of the Oz axis. The magnetization vector is oriented along the field and the same negative direction of the axis.

At the initial moment, static field H_0 is switched from the negative to positive direction, so that the magnetization becomes opposite to the external field. The equilibrium of the magnetization along the direction that is opposite to the field is unstable, and minor transverse fluctuations of the magnetization vector can lead to the rotation of this vector toward the direction of the field (i.e., the positive direction of the Oz axis). Thus, the magnetization is orientationally switched from negative to positive direction of the Oz axis. Owing to the gyrotropic properties of the magnetic medium, the magnetization vector exhibits the helical motion [17]. Such motion induces similar motion of the elastic displacement owing to the magnetostrictive effect, so that the hypersonic oscillations are excited.

We consider the development of oscillations of magnetization and elastic displacement that result from the activation of the static magnetic field. Figure 2 illustrates

the general scenario and presents the time dependences of the normalized components of magnetization m_x and m_z, displacement u_x and precession portraits of magnetic $m_y(m_x)$ and elastic $u_y(u_x)$ oscillations.

In the calculations, we employ the material parameters that are typical of the YIG single crystal: $4\pi M_0 = 1750$ G, $B_2 = 6.96 \times 10^6$ erg cm^{-3}; $c_{44} = 7.64 \times 10^{11}$ erg cm^{-3}, and $\rho = 5.17$ g cm^{-3}. The curves are well resolved when the orientation transition corresponds to no greater than 30–50 periods of oscillations. Thus, we choose the following decay parameters of the magnetic and elastic subsystems: $\alpha = 0.05$ and $\beta = 10^{11}$ s^{-1}, which are slightly greater than the values typical of the YIG crystal ($\alpha = 0.001$ and $\beta = 10^6$ s^{-1}). For such decay parameters, the relaxation times are $\tau_m = 0.114 \times 10^{-8}$ s and $\tau_e = 0.001 \times 10^{-8}$ s for magnetic and elastic oscillations, respectively. The remaining parameters are chosen in such a way that the resonance frequencies of the uniform precession and the first mode of elastic oscillations coincide for the linear oscillations in the absence of magnetoelastic coupling (the frequencies are 2800 MHz and the corresponding period is 3.571×10^{-10} s). In this case, the static field is 2750 Oe and the thickness of the magnetic plate is 0.6865 μm. The initial components of the normalized magnetization are $m_{xs} = 7 \times 10^{-5}$, $m_{ys} = 0.00$, and $m_{zs} = -1.00$. The initial components of the elastic displacement are zeros. We consider the development of oscillations at time interval $0-10^{-8}$ s with a step of $\Delta t = 10^{-12}$ s. The fourth-order Runge–Kutta procedure is employed [18].

We detect elastic oscillations on the surface of the magnetic plate at $z = d/2$. The opposite-phase oscillations with the same amplitude are observed at $z = -d/2$.

Figure 2 illustrates the development of magnetic and elastic oscillations. The inset to Fig. 2b shows the scheme of sequential variations in the orientation of magnetization vector.

Typical times that correspond to the minimum amplitudes of magnetic oscillations t_g and t_h (Fig. 2c) are measured at a level of 0.01 of unity. Typical times of elastic oscillations t_k and t_p (Fig. 2e) are measured at a level of 0.05×10^{-10} cm. At time moments t_a and t_c (Fig. 2a), quantity m_z differs from unity by 0.01.The characteristic times are

Time instant	$t \times 10^{-8}$, s
t_a	0.17
t_b	0.26
t_c	0.56
t_g	0.10
t_h	0.88
t_k	0.09
t_m	0.24
t_n	0.32
t_p	0.97

We use the above data in a detailed analysis of variations in magnetization and elastic displacement in the course of orientation transition.

3. STABILIZATION OF MAGNETIZATION IN ORIENTATION TRANSITION

The time dependence of quantity m_z (Fig. 2a) and the scheme of sequential variations in the orientation of magnetization vector (Fig. 2b) illustrate the stabilization of magnetization in the orientation transition. At the initial and final moments, the magnetization is oriented along the negative and positive directions of the Oz, axis, respectively.

Figure 2a shows that the rotation of the magnetization vector is started with delay t_a relative to the activation of the field. Magnetization vector passes through the Oxy plane at moment t_b and almost reaches the positive direction of the Oz axis at moment t_c. The times of the first and second parts of the rotation are $t_b - t_a = 0.07 \times 10^{-8}$ s and $t_c - t_b = 0.23 \times 10^{-8}$ s, respectively. The difference between the time intervals is due to the fact that the force providing the rotation of the magnetization vector toward the field increases at the first stage when the deviation of the magnetization vector from the field direction increases. At the second stage, the deviation and, hence the force decrease to zero. Therefore, the first stage of the orientation transition is shorter than the second stage.

An important feature of the orientation transition lies in the fact that the rotation of the magnetization vector is delayed relative to starting moment $t = 0$, and the delay ($t = t_a = 0.17 \times 10^{-8}$ s) is comparable with the time of the remaining part of the transition $t_c - t_a = 0.39 \times 10^{-8}$ s. Below we analyze such a delay.

4. MAGNETIC OSCILLATIONS

A variation in the orientation of the magnetization vector is accompanied by its precession around the Oz. axis owing to the gyrotropic properties of the magnetic medium. Figure 2c shows that the magnetic oscillations are started at moment t_g, which is slightly less than t_a, and are terminated at moment t_h, which is greater than t_c. Such a difference is due to the fact that transverse component of magnetization m_x is no greater than 0.2 at time intervals between t_g and t_a and between t_c and t_h, so that the longitudinal component of magnetization is $m_z = \pm 0.96$ (i.e., such variations are insignificant in Fig. 2a). The magnetic oscillations reach maximum at moment t_b when the magnetization vector passes through the plane. Such motion corresponds to full-scale circular precession on the Oxy plane.

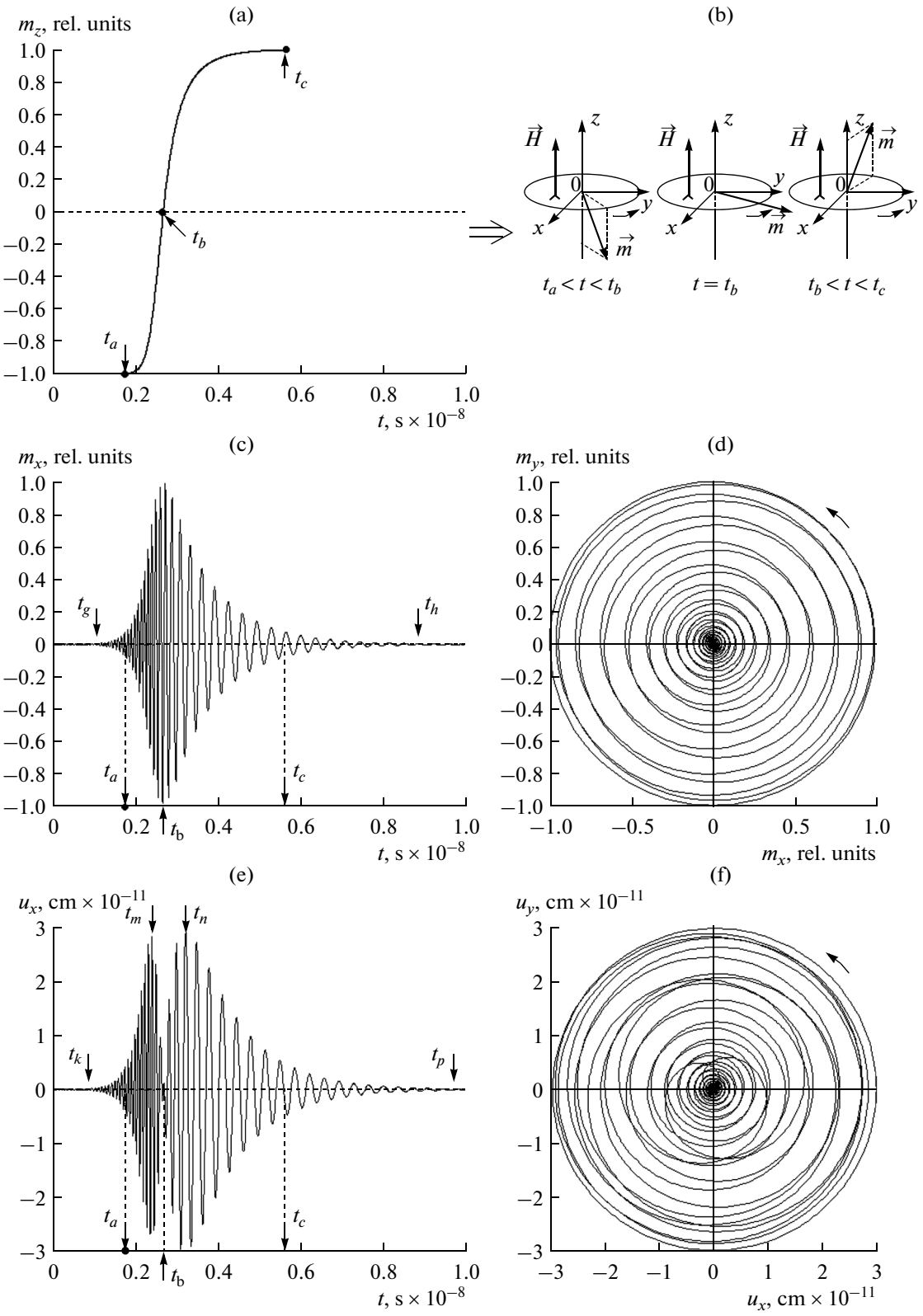

Fig. 2. Plots of normalized components of magnetization (a) m_z and (c) m_x and (e) displacement u_x vs. time, precession portraits of (d) magnetic m_y (m_x) and (f) elastic u_y (u_x) oscillations, and (b) scheme of reorientation of the magnetization vector (see table for characteristic times of the processes).

Figure 2c shows that the period of magnetic oscillations (about 0.87×10^{-10} s) is significantly less than the resonance period when the full-scale precession is not reached. However, the period increases and becomes equal to the resonance period (3.57×10^{-10} s) after several (three or four) oscillations when the maximum is reached at moment t_b.

Such evolution of the period is due to the fact that both external and demagnetization fields are exerted along the same direction (the positive direction of the Oz axis) when the oscillations take place in the lower half-plane, whereas the external and demagnetization fields are exerted along the positive and negative directions of the Oz axis, respectively, in the upper half-plane. The precession frequencies in the lower and upper half-planes are given by [19]

$$\omega = \gamma\left(H_0 + 4\pi M_0\right), \tag{12}$$

$$\omega = \gamma\left(H_0 - 4\pi M_0\right), \tag{13}$$

respectively.

The periods that are calculated using these formulas (0.79×10^{-10} and 3.57×10^{-10} s, respectively) are in good agreement with the values in Fig. 2c.

Figure 2c shows the oscillations of only x component of the magnetization vector, since the y component exhibits similar oscillations that are phase-shifted by 90°. Under such conditions the phase portrait in Fig. 2d represents almost regular concentric rings. The concentration of the trajectories on the portrait in the vicinity of zero corresponds to the initial stage of oscillations up to moment t_a when the variations in amplitude are relatively slow and the period is significantly less than the resonance period.

Figure 2c shows that the magnetic oscillations are delayed relative to starting moment $t = 0$ and the delay is $t_g = 0.10\times10^{-8}$ s. Such a delay is similar to the delay of the rotation of the magnetization vector (Fig. 2a). A minor difference between times t_a and t_g is apparently due to insufficient measurement accuracy of the initial levels of both processes.

5. ELASTIC OSCILLATIONS

In the presence of magnetostriction, the oscillations of magnetization induce the oscillations of elastic displacement (Fig. 2e). Elastic oscillations are started at moment t_k that is close to t_a and evolve in two stages: first, the oscillations emerge with a period (0.87×10^{-8} s) that is equal to the period of magnetic oscillations and an amplitude that increases and reaches a maximum level of 3×10^{-11} cm at moment t_m, then, the amplitude decreases to zero at moment t_b. After that, the amplitude sharply increases and reaches a level of 3.0×10^{-11} cm at moment t_n. Then, the amplitude gradually decreases and tends to zero at moment t_p, which is substantially greater than t_c.

The comparison of Figs. 2c and 2d shows that the decay of elastic oscillations at time greater than t_n takes place with the time constant (0.114×10^{-8} s) that is equal to the decay time of magnetic oscillations. The reason for such equality lies in the fact that relaxation time of elastic oscillations τ_e is significantly less than relaxation time of magnetic oscillations τ_m for the above decay parameters, so that elastic oscillations follow the magnetic oscillations in the quasi-stationary regime. When the elastic oscillations are induced, their period follows the period of magnetic oscillations also due to the quasi-stationary character of the process. In our opinion, a delay in the development of the elastic oscillations up to moment $t_k = 0.09\times10^{-8}$ s is caused by the same reason as a similar delay of magnetic oscillations is, since the elastic oscillations completely reproduce the magnetic oscillations at the above decay parameters.

Note almost regular shapes of the precession portraits, which indicate identity of elastic oscillations with respect to the x and y axes with a phase shift of 90°. The concentration of the trajectories in the vicinity of zero also corresponds to the initial stage of oscillations where the period is less than the resonance period.

An important difference between the elastic and magnetic oscillations is the amplitude minimum at moment t_b, where the magnetization vector passes through the Oxy plane and its precession occurs in this plane. Below, we analyze this minimum.

6. MINIMUM OF ELASTIC DISPLACEMENT

Formula (51) from [15] shows that the x component of elastic displacement in the approximation of the first elastic mode is represented as

$$u_x = -\frac{B_2}{c_{44}} m_x m_z z + v_x \sin\left(\frac{\pi}{d} z\right), \tag{14}$$

where v_x is auxiliary function that satisfies the following equation (see formula (53) in [15]):

$$\frac{\partial^2 v_x}{\partial t^2} + 2\beta\frac{\partial v_x}{\partial t} + \frac{c_{44}\pi^2}{\rho d^2} v_x = \frac{4B_2 d}{c_{44}\pi^2}\left[\frac{\partial^2}{\partial t^2}\left(m_x m_z\right) + 2\beta\frac{\partial}{\partial t}\left(m_x m_z\right)\right]. \tag{15}$$

On the surface of the magnetic plate ($z = d/2$), displacement (14) is represented as

$$u_x = -\frac{B_2 d}{2c_{44}} m_x m_z + v_x. \tag{16}$$

We assume that variations in m_z are significantly slower than variations in m_x and v_x. Control estima-

tions show that such a relationship is satisfied more accurately when both decays are slower. We assume that quantity m_z remains constant and the magnetization and elastic displacement are represented as

$$m_x = m_{xc}\exp(i\omega t); \quad (17)$$

$$v_x = v_{xc}\exp(i\omega t). \quad (18)$$

Then, Eq. (15) is represented as

$$-\omega^2 v_{xc} + 2i\beta\omega v_{xc} + \frac{c_{44}\pi^2}{\rho d^2} v_{xc} = \frac{4B_2 d}{c_{44}\pi^2}\left(\omega^2 m_{xc}m_{zc} + 2i\beta\omega m_{xc}m_{zc}\right). \quad (19)$$

Thus, we obtain

$$v_{xc} = \frac{\left(4B_2 d/c_{44}\pi^2\right)\omega(\omega + 2i\beta)}{-\omega^2 + 2i\beta\omega + \left(c_{44}\pi^2/\rho d^2\right)} m_{xc}m_{zc}. \quad (20)$$

Substituting this expression in formula (16), we derive

$$u_x = -\frac{B_2 d}{2c_{44}}\left\{1 - \frac{\frac{8}{\pi^2}\omega(\omega + 2i\beta)}{-\omega^2 + 2i\beta\omega + \frac{c_{44}\pi^2}{\rho d^2}}\right\} m_{xc}m_{zc}. \quad (21)$$

We do not analyze the structure of this expression but it is seen that the elastic displacement is related to the components of the magnetization:

$$u_x = Am_{xc}m_{zc}. \quad (22)$$

Here, A is time-independent constant.

Therefore, the elastic displacement reaches minimum when the magnetization vector passes through the Oxy plane (i.e., magnetization component m_z is zero). However, quantity u_x differs from zero on both sides of the minimum and repeatedly tends to zero when the magnetization is oriented along the Oz axis (i.e., transverse component of magnetization m_x is close to zero). Thus, the dependence of amplitude u_x of elastic displacement on time must tend to zero at moments t_g and t_h and be equal to zero at moment t_b.

Note also that the amplitude of elastic displacement is proportional to magnetization component m_x and exhibits resonance dependence on frequency in accordance with expression (21).

7. EMPIRICAL MODEL BASED ON EXPONENTIAL FUCNTIONS

Figure 2 shows similarity of time dependences of magnetic and elastic oscillations. Thus, we employ an approximation in which the envelopes of both dependences are described using identical exponential functions and construct an empirical model of such dependences.

We assume that the envelopes of the time dependences of the normalized components of magnetization and elastic displacement can be approximately represented as

$$m_{z0}(t) = \exp\left[\varepsilon_1(t - t_b)\right] - 1; \quad (23)$$

$$m_{x0}(t) = \exp\left[\delta_1(t - t_b)\right]; \quad (24)$$

$$u_{x0}(t) = \exp\left[\eta_1(t - t_b)\right] \quad (25)$$

at $t \geq t_b$ and

$$m_{z0}(t) = -\exp\left[\varepsilon_2(t - t_b)\right] + 1; \quad (26)$$

$$m_{x0}(t) = \exp\left[\delta_2(t - t_b)\right]; \quad (27)$$

$$u_{x0}(t) = \exp\left[\eta_2(t - t_b)\right] \quad (28)$$

at $t \geq t_b$.

Coefficients in the exponents that are calculated using amplitudes m_z, m_x, and u_x at moments t_a, t_b, t_c, t_h, and t_p are

$$\varepsilon_1 = 5.1169\times10^9\ \text{s}^{-1}; \quad \delta_1 = 2.8782\times10^9\ \text{s}^{-1};$$

$$\varepsilon_2 = -1.5351\times10^9\ \text{s}^{-1}; \quad \delta_2 = -7.4277\times10^8\ \text{s}^{-1};$$

$$\eta_1 = 3.0701\times10^9\ \text{s}^{-1}; \quad \eta_2 = -7.0849\times10^8\ \text{s}^{-1}.$$

The solid lines in Fig. 3 show the time dependences of the envelopes of magnetization and elastic-displacement components that are calculated using the above formulas. The dashed lines show the same dependences that are calculated with the aid of equations of motion.

It is seen that the empirical dependences coincide with the dependences that result from the solution to the general problem with an accuracy of several percents.

8. MODEL OF THE QUASI-STATIC ROTATION OF THE MAGNETIZATION VECTOR

In accordance with the configuration of the problem, the field is directed along the positive direction of the Oz axis. In the initial state, the magnetization vector is opposite to the field (i.e., directed along the negative direction of the axis). At a minor deviation from the Oz axis, the force that is exerted on the magnetization vector provides the rotation of this vector from negative to positive direction. The orientation transition involves such a rotation. We consider a relatively slow quasi-static rotation in which the gyrotropic properties of the magnetization vector are not manifested and it rotates in the plane that contains the Oz axis as a magnetic dipole that contains two charges.

We use a coordinate system whose Oxz plane coincides with the plane of rotation of the magnetization vector.

We also introduce a spherical coordinate system whose polar axis coincides with the Oz axis and the azimuth angle is counted from the Ox axis. The Carte-

sian components of normalized magnetization vector $\vec{m}$ that rotates in the Oxz plane are represented as

$$m_x = \sin\theta; \quad (29)$$

$$m_y = 0; \quad (30)$$

$$m_z = \cos\theta, \quad (31)$$

where θ is the polar angle of vector $\vec{m}$ (the angle between this vector and the Oz axis).

In the presence of the field, the moment that is exerted on the magnetization vector is written as [20, 21]

$$\vec{P} = \left[\vec{M} \times \vec{H}\right]. \quad (32)$$

The configuration of the problem shows that this moment is directed along the Oy axis. Based on the properties of the vector product, we obtain

$$P = M_0 H \sin\theta. \quad (33)$$

In accordance with the law of rotational motion [22], we have

$$P = J\left(d\omega/dt\right), \quad (34)$$

where J is the moment of inertia and ω is the angular velocity.

The angular velocity of the magnetization vector is related to polar angle θ:

$$\omega = d\theta/dt. \quad (35)$$

Substituting expressions (33) and (35) in formula (34), we derive the following equation for time variations in angle θ:

$$\frac{d^2\theta}{dt^2} - G\sin\theta = 0, \quad (36)$$

where

$$G = M_0 H/J. \quad (37)$$

In general, we obtain a periodic solution to this equation but we consider only the time interval that corresponds to one half of the first period, since the magnetization vector is reoriented over this interval. In the absence of an exact expression for the moment of inertia of the magnetization vector, we choose coefficient G in such a way that a variation in the longitudinal component of normalized magnetization vector m_z given by Eq. (36) is almost identical to a variation that is calculated using Eqs. (2)–(11). Figure 4 demonstrates the corresponding solution to Eq. (36). Figure 4a shows extremely slow rotation of the magnetization up to moment t_a, since the rotating force is small in the vicinity of the antiparallel orientation of the magnetization and field. Then, the rotating force increases in the interval from t_a to t_d when the magnetization is reoriented. The most significant variations correspond to the transition through the Oxy plane (moment t_b) when the rotating force reaches maximum. After moment t_d, the rotation becomes slower

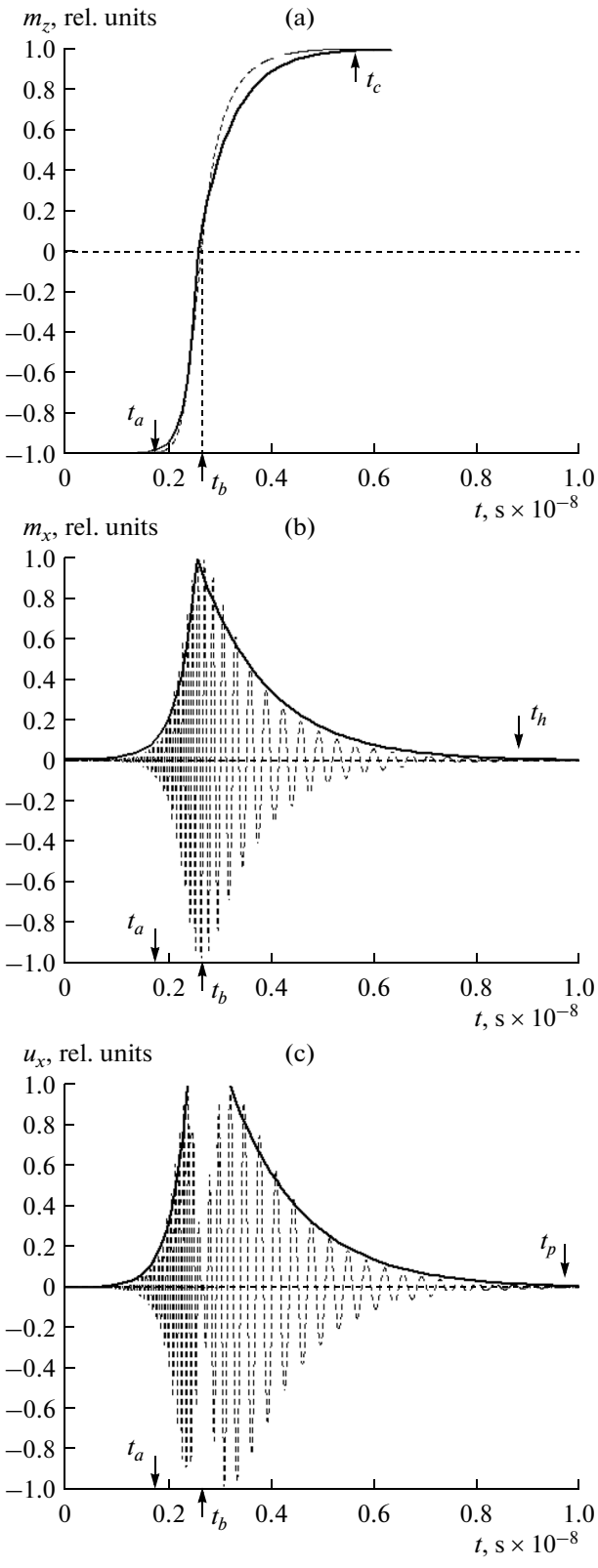

Fig. 3. Curves of (a) and (b) components of magnetization vector and (c) elastic displacement vs. time that are calculated using (solid lines) exponential approximation and (dashed lines) equations of motion (see table for characteristic times of the processes).

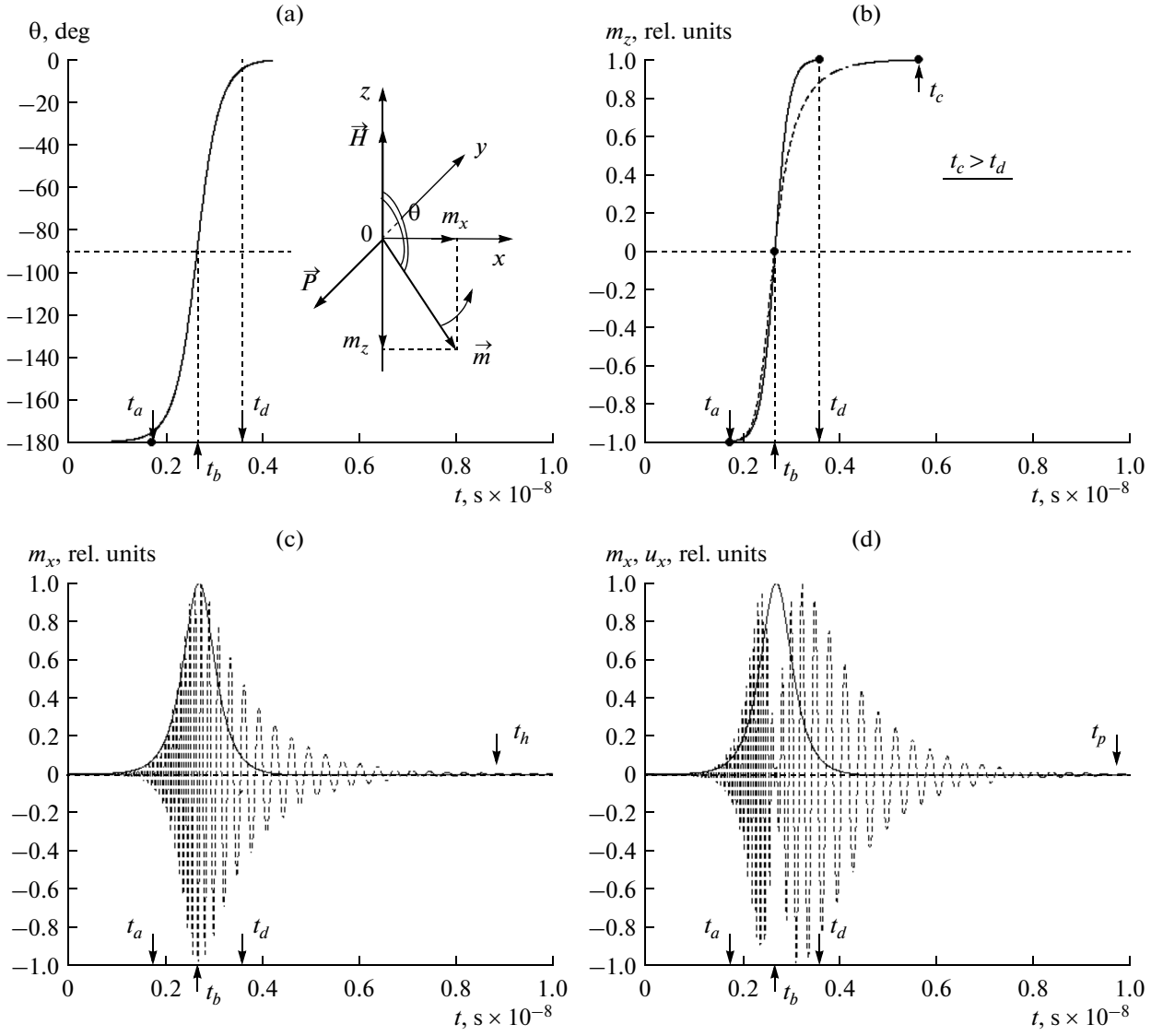

Fig. 4. Curves of (a) orientation angle, (b) and (c) components of magnetization vector, and (d) elastic displacement vs. time that are calculated using (solid lines) the model of quasi-static rotation and (dashed lines) equations of motion. The inset to panel (a) shows the scheme of rotation of the magnetization vector. The model parameters are $G = 1.2 \times 10^{-8}$ s^{-2}, $m_{x0} = 7 \times 10^{-4}$ (initial displacement) and $t_a = 0.20 \times 10^{-8}$ s (see table for the remaining characteristic times of the processes).

and the magnetization direction slowly reaches the field direction, since the rotating force decreases and tends to zero at the parallel orientation of the magnetization and field. Note symmetric dependence $\theta(t)$ with respect to point t_b, so that $t_b - t_a = t_d - t_b$.

The solid line in Fig. 4b shows the dependence of longitudinal component of magnetization m_z that is calculated using dependence $\theta(t)$ (Fig. 4a). The dashed line shows the corresponding dependence that is calculated with the aid of equations of motion (2)–(11). It is seen that the dependences almost coincide in time interval from t_a to t_b. Then, the dependence that is calculated using the equations of motion becomes substantially slower and the value $m_z = 1$ is reached only at moment t_c. Note asymmetric dependence $m_z(t)$ with respect to point t_b: $t_b - t_a < t_c - t_b$.

The solid line in Fig. 4c shows the dependence of transverse component of magnetization m_x that is calculated using dependence $\theta(t)$ (Fig. 4a). Similarly to the remaining curves that are calculated using the model, this curve is symmetric with respect to point t_b. The dashed line shows the corresponding dependence that is calculated using the equations of motion. Note the absence of symmetry in this case. In the time interval from t_a to t_b, the curve that is calculated using the model of quasi-static rotation corresponds with a relatively high accuracy to the envelope of the positive half-periods of the dependence that is calculated using the

equations of motion. Then, the curve that is calculated with the aid of equations of motion becomes substantially slower and approaches zero only at moment t_h, which is significantly greater than t_d ($(t_h - t_b)/(t_d - t_b) \approx 10$).

The solid line in Fig. 4d shows the dependence of the transverse component of magnetization m_x that is calculated from dependence $\theta(t)$ (Fig. 4a). The dashed line shows the dependence of transverse component of elastic displacement u_x that is calculated using equations of motion and normalized to unity. Up to moment t_b, dependence m_x reasonably coincides with the envelope of the positive peaks of curve u_x. Then, dependence u_x and a similar dependence of the magnetic component (Fig. 4c) become significantly slower and tend to zero at moment t_p, which is significantly greater than t_d and close to t_h, so that $(t_p - t_b)/(t_d - t_b) \approx 11$.

Thus, we conclude that the model of the quasi-static rotation reasonably well describes the envelope of oscillations at the first stage of the rotation of magnetization toward the Oxy plane. Then, the decay of oscillations becomes substantially slower and the decay time that is calculated using the model is less by a factor of 10–11.

Slower decays of quantities $m_x(t)$ and $u_x(t)$ in comparison with the decay of quantity $m_z(t)$ that is calculated with the aid of the model of quasi-static rotation can be due to the following reasons. The magnetization vector rotates under the action of an increasing force in the interval from t_a to t_b and directly follows the force, since it is relatively large. Then, the force decreases and the motion of the magnetization vector becomes close to the free motion and the corresponding decay is determined by the natural relaxation time (i.e., the time of a decrease by a factor of $e = 2.718\ldots$ is $\tau_m = 0.114 \times 10^{-8}$ s). (Figure 2e shows that the time of a decrease to a level of about 0.37 is 0.12×10^{-8} s.) Such almost free motion causes an increase in time t_h relative to time t_d. In this case, the elastic oscillations almost follow the magnetic oscillations owing to the smallness of the relaxation time of elastic oscillations in comparison with the magnetic relaxation time ($\tau_e \ll \tau_m$). Thus, time t_p is significantly greater than time t_d.

9. DEPENDECNE OF THE LONGITUDINAL COMPONENT OF MAGNETIZATION ON MAGNETIC DECAY PARAMETER

We consider the dependences of the characteristic times of magnetization and elastic-displacement components on the corresponding decay parameters and the initial deviation of the magnetization vector from the field direction.

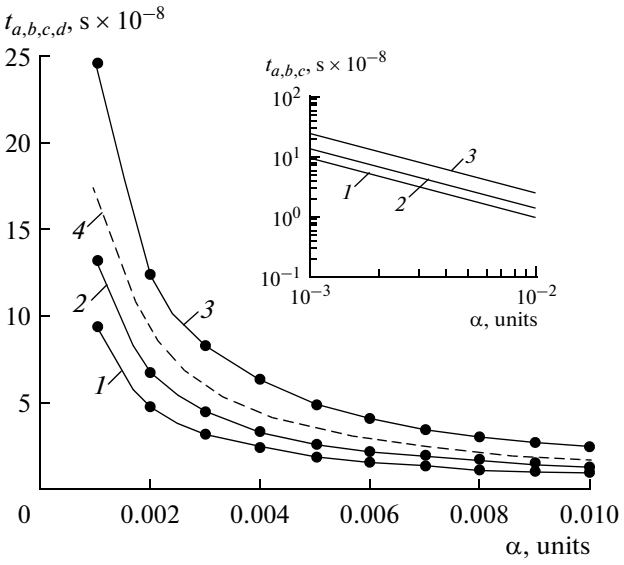

Fig. 5. Plots of characteristic times (*1*) t_a, (*2*) t_b, (*3*) t_c, and (*4*) t_d of variations in longitudinal component of magnetization m_z vs. magnetic decay parameter α for the parameters of Fig. 4 (the dots show the results of computer experiments). The inset shows the same curves on the double logarithmic scale.

Figure 5 presents the dependences of characteristic times t_a, t_b, and t_c of longitudinal components of magnetization m_z on magnetic decay parameter α.

We use the following criteria in the calculations of the characteristic times. At moment t_a (curve *1*), magnetization component m_z differs from −1 by 0.01 (i.e., m_z is −0.99) and the amplitude of magnetic oscillations m_x is 0.01. At moment t_b (curve *2*) magnetization component m_z passes through zero and amplitude of magnetic oscillations m_x reaches a maximum level of 1.00. At moment t_c (curve *3*) magnetization component m_z differs from unity by 0.01 (i.e., m_x is 0.99) and the amplitude of magnetic oscillations m_x decreases by about an order of magnitude relative to the maximum level (i.e., m_x is about 0.1). At moment t_d (curve *4*), magnetization component that is calculated using the model of quasi-static rotation is $m_z = 0.99$.

Figure 5 shows that the characteristic times decrease with an increase in the magnetic decay. Such a decrease is clearly manifested at small α that are close to the decay parameter of YIG (0.001). Note a linear curve on the double logarithmic scale (see inset). Control calculations show that the linearity is maintained when parameter α ranges from 0.001 to 0.005 (i.e., the entire range of magnetic decay typical of ferrite materials).

Figure 5 also shows that delay time $t_c - t_d$ needed for the alignment of magnetization along the Oz axis increases with a decrease in quantity α. This result fol-

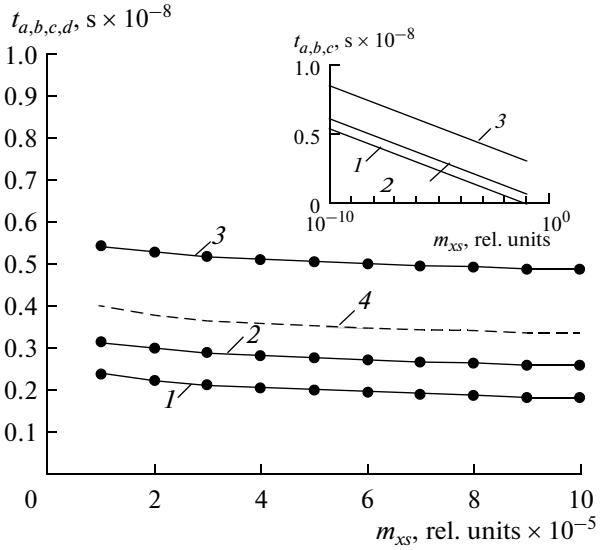

Fig. 6. Plots of characteristic times (*1*) t_a, (*2*) t_b, (*3*) t_c, and (*4*) t_d of variations in longitudinal component of magnetization m_z vs. initial transverse magnetization m_x for the parameters of Fig. 4 (the dots show the results of computer experiments). The inset shows the same curves on the logarithmic scale.

lows from the fact that the magnetization acquires a unity amplitude when it passes through the Oxy plane and the precession is started. The greater parameter α, the longer the precession (the slower a decrease in the transverse components of magnetization). The longitudinal component is determined by the difference between unity and a sum of squares of transverse components. Therefore, the longitudinal component slowly approaches unity when the transverse components exhibit a slow decay. Thus, the difference between time t_c and t_d increases when decay parameter α decreases.

10. DEPENDENCE OF THE LONGITUDINAL COMPONENT OF MAGNETIZATION ON THE INITIAL VALUE OF ITS TRANSVERSE COMPONENT

Figure 6 presents the dependences of characteristic times of variations in longitudinal component of magnetization m_z on the initial transverse component of magnetization m_{xs}. The characteristic times are counted as in the previous case.

It is seen that the characteristic times decrease with an increase in the initial transverse component of magnetization and the decrease is more developed at smaller m_{xs}. Note linearity of the curves that are plotted on the logarithmic scale of the horizontal axis (see inset) in the interval 10^{-10}–0.1, which corresponds to real ferrite materials at technically feasible temperatures.

Figure 6 also shows that delay time $t_c - t_d$ of the alignment of magnetization along the Oz axis remains unchanged in the entire interval of variation in initial magnetization m_x. This result is due to the fact that the conditions for the orientation transition, which are determined by the initial and final positions of the magnetization vector and external field, remain unchanged. At any initial displacement, the rotation rate of magnetization is determined only by the gyrotropic properties of the material and the external field.

11. RELATIONSHIP OF THE MAXIMUM AMPLITUDES OF MAGNETIC AND ELASTIC OSCILLATIONS AND DECAY PARAMETERS

We consider the relationship of the maximum amplitudes of magnetic and elastic oscillations and magnetic α and elastic β decay parameters.

When the reorientation takes place, magnetization vector always passes through the Oxy plane. Therefore, the maximum transverse component of the magnetization always passes through unity regardless of the magnetic and elastic decay parameters. Thus, the magnetic oscillations are always started from unity after passage through the plane and the maximum amplitude of the oscillations does not depend on the decay parameters.

At a relatively high elastic decay when the elastic oscillations follow the magnetic oscillations with a relatively high accuracy, the maximum amplitude of elastic oscillations also does not depend on the magnetic decay. This conclusion is verified for parameter α ranging from 0.001 to 0.5. In particular, the maximum amplitude of elastic oscillations is 3×10^{-1} cm with an accuracy of about 1% in the entire interval of variations in parameter α when the elastic decay parameter is $\beta = 10^{11}$ s^{-1}. Such independence of the amplitude of elastic oscillations on magnetic decay parameter α is also obtained when elastic decay parameter β ranges from 10^6 to 10^{11} s^{-1}.

However, such a conclusion is valid only for magnetic oscillations whereas the amplitude of elastic oscillations is not related to a characteristic quantity that reaches a limiting level in the course of orientation transition. Thus, the amplitude of elastic oscillations may exhibit significant variations (see below) when elastic decay parameter β is varied.

12. SPECIFIC FEATURES OF THE EXCITATION OF HYPERSOUND AT RELATIVELY LOW ELASTIC DECAY

The above analysis of the excitation of hypersound due to orientation transition with respect to magnetization is valid for a significant decay of the elastic oscillations. In this case, the elastic oscillations follow the oscillations of magnetization. Consider specific

features of the effect at lower decay of elastic oscillations.

Figure 7 shows the time dependences of normalized components of magnetization m_x and m_z (panel (a)) and displacement u_x (panel (b)) for decay parameter $\beta = 10^9\ \text{s}^{-1}$, which is less than decay parameter $\beta = 10^{11}\ \text{s}^{-1}$ for which similar curves are plotted in Fig. 2 by two orders of magnitude.

The comparison of Figs. 7 and 2 shows that the magnetic oscillations remain almost unchanged (Fig. 7a is almost identical to Fig. 2a) when the decay parameter of elastic oscillations decreases by two orders of magnitude. However, the elastic oscillations are substantially modified (Fig. 7b): the maximum amplitude increases by approximately an order of magnitude and the envelope of elastic oscillations appears to be significantly delayed relative to the magnetic envelope. In particular, time t_n, which corresponds to the maximum of elastic oscillations, increases by $\Delta t_p = 0.15\times10^{-8}$ s and time t_p, which corresponds to a decrease in the amplitude to a level of 0.01 of maximum, increases by $\Delta t_p = 0.31\times10^{-8}$ s (i.e., the development of elastic oscillations is delayed relative to the development of magnetic oscillations).

We assume that such a delay is due to the resonance properties of the elastic oscillatory system that become more significant when the decay decreases. Indeed, the maximum level of oscillations is reached in any oscillation system after the excitation with a delay determined by the relaxation time, which is inversely proportional to the decay parameter. In the system under study, the amplitude of elastic oscillations must decrease by a factor of $e = 2.71828...$ at a time of $\tau_e = \beta^{-1}\ \text{s} = 10^{-9}$ s but the direct measurements in the time interval from 0.6×10^{-8} to 0.8×10^{-8} s show that the amplitude of elastic oscillations decreases in such a way in a time interval of 1.55×10^{-9} s, which is slightly greater than the above estimated time. Such a difference can be due to the fact that the elastic oscillations that are induced by magnetic oscillations are partly sustained due to the latter, so that the effective decay parameter of elastic oscillations slightly decreases.

On the other hand, the delay time of the maximum of elastic oscillations relative to the maximum of magnetic oscillations is $t_n - t_b = 0.21\times10^{-8}$ s, which is also greater than the above value. Apparently, such a delay results from the fact that amplitude of magnetic oscillations decreases after moment t_b, at which the maximum is reached (i.e., elastic oscillations are excited by decaying magnetic oscillations).

Time t_p that corresponds to a decrease in the elastic oscillations to a level of 0.01 of the maximum is substantially greater than similar time t_h, which characterizes a decrease in the magnetic oscillations, so that the difference amounts to $t_p - t_h = 0.40\times10^{-8}$ s. We assume that such a difference is related to the free decay of elastic oscillations, which is almost independent of magnetic oscillations. Indeed, the time of exponential decrease in the oscillation amplitude from 1.00 to 0.01 at a decay parameter of $\beta = 10^9\ \text{s}^{-1}$ is 0.41×10^{-8} s, which is in good agreement with the result of measurements.

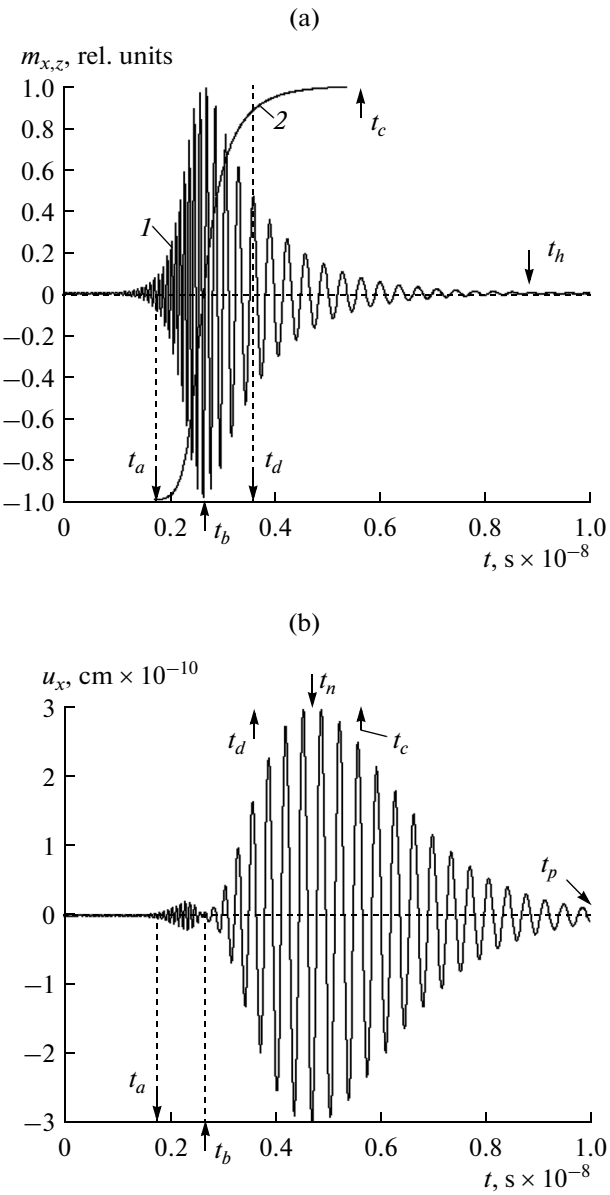

Fig. 7. Curves of (a) normalized components of magnetization vector (*1*) m_x and (*2*) m_z and (b) displacement u_x vs. time for decay parameter $\beta = 10^9\ \text{s}^{-1}$ and characteristic times $t_d = 0.32\times10^{-8}$ s, $t_n = 0.47\times10^{-8}$ s, and $t_p = 1.28\times10^{-8}$ s (see text for the remaining characteristic times).

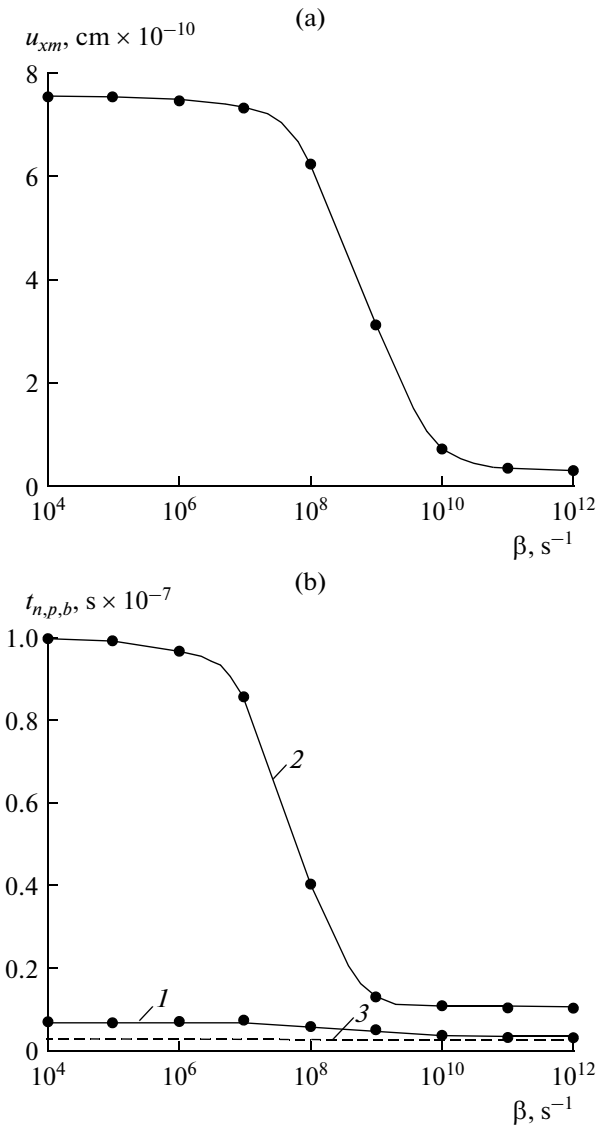

Fig. 8. Plots of (a) amplitude and (b) characteristic times (*1*) t_n, (*2*) t_p, and (*3*) t_b of elastic oscillations vs. decay parameter.

13. DEPENDECES OF AMPLITUDE AND CHARACTERISTIC TIMES OF THE DEVELOPMENT OF ELASTIC OSCILLATIONS ON DECAY PARAMETER

We consider specific features of the excitation of elastic oscillations at different decay parameters β. Figure 8 demonstrates the corresponding dependences for maximum amplitude u_{xm} and characteristic times of elastic oscillations t_n, t_p, and t_b. For convenience, the curves are plotted on the logarithmic scale of the horizontal axis.

Figure 8 shows that the maximum amplitude (Fig. 8a) and characteristic times (Fig. 8b) remain almost unchanged at $\beta < 10^5$ s^{-1} and $\beta > 10^9$ s^{-1}. However, all of the quantities strongly decrease in the interval 10^5 $s^{-1} \le \beta \le 10^9$ s^{-1}. Note that characteristic time t_b (curve *3* in Fig. 8b), at which the magnetization vector passes through the *Oxy* plane remains constant (i.e., independent of elastic decay).

The constancy of amplitudes and characteristic times outside the above interval can be due to the following reasons. At relatively small parameter β ($\beta < 10^5$ s^{-1}), the decay of elastic oscillations is insignificant and depends on magnetic (independent of β) rather than elastic loss. At relatively large parameter β ($\beta > 10^9$ s^{-1}), the elastic oscillations become almost aperiodic and the amplitude of elastic displacements follows the transverse magnetization, so that the decay of elastic oscillations is also determined by the magnetic decay. In the above interval 10^5 $s^{-1} \le \beta \le 10^9$ s^{-1}, the elastic decay dominates over the magnetic decay and amplitude u_{xm} and times t_n and t_p exhibit significant variations.

Note that time t_p is significantly greater than time t_n at small β, so that the elastic oscillations slowly decay almost in the absence of contribution of the magnetic oscillations.

14. REMARKS ON PRACTICAL APPLICATIONS

The curves in Fig. 8 are plotted for a relatively large magnetic decay parameter α = 0.05, whereas the decay parameter of YIG is significantly less (0.001). YIG is the most promising material for hypersonic excitation in practice, since it exhibits record-low magnetic and elastic losses. Therefore, it is expedient to determine the limiting parameters of the excited hypersound in this material.

For the real parameters of YIG (α = 0.001 and β = 10^6 s^{-1}), initial value $m_{xs} = 7 \times 10^{-5}$, and magnetic field of 2750 Oe, which corresponds to a frequency of 2800 MHz, we obtain the following characteristic times: $t_a = 0.06 \times 10^{-6}$ s, $t_b = 0.10 \times 10^{-6}$ s, $t_n = 0.24 \times 10^{-6}$ s, and $t_p = 1.12 \times 10^{-6}$ s. The amplitude of the excited hypersound is $u_{xm} = 0.995 \times 10^{-9}$ cm, which is greater than the amplitude in [15] by a factor of greater than 2, and the excitation is higher than linear by three-to-four orders of magnitude.

CONCLUSIONS

The main results are as follows.

Using the configuration of a normally magnetized ferrite plate that exhibits magnetoelastic properties, we consider the dynamic behavior of the magnetization vector related to the orientation transition from the direction that is antiparallel to the static field via the plate plane to the parallel direction.

Such a reorientation of the magnetization vector is accompanied by its precession around the field direction. Prior to and after the moment when the magnetization vector passes through the plate plane, the precession frequency is determined by a sum of the external and demagnetization fields and the difference of the fields, respectively.

The reorientation of the magnetization due to magnetostriction causes the excitation of high-intensity hypersonic elastic oscillations whose frequency corresponds to the precession frequency of the magnetization vector in the presence of the magnetization reversal. When the magnetization vector is far from the plate plane, the amplitude of elastic oscillations is proportional to the precession amplitude. When the magnetization vector passes through the plate plane, the elastic amplitude is zero.

The rotation of the magnetization vector and the development of elastic oscillations are delayed relative to the field switching, and the delay time is proportional to the relaxation time of magnetic oscillations and inversely proportional to the initial deviation of the magnetization vector from the field direction.

At a relatively small decay parameter of elastic oscillations, the development of such oscillations can also be delayed relative to the development of magnetic oscillations determined by the magnetic relaxation time.

We obtain longer decays of magnetic and elastic oscillations after termination of field switching, which are determined by a decrease in the force that provides the rotation of the magnetization vector toward the field direction with a decrease in the angle between the two vectors.

Two models are proposed for interpretation of the effects. An empirical model describes the development of oscillations using exponential approximation, and a vector model is based on the quasi-static rotation of the magnetization vector relative to the field direction. The accuracy of the exponential approximation of the amplitude envelopes is several percents when the magnetic and elastic oscillations depend on time. The model of the rotation allows a high-accuracy analysis of an increase in the oscillation amplitude prior to the moment when the magnetization vector passes through the plane. However, the results of the model are slightly delayed relative to the observed decrease in the amplitude after passage through the plane. The delay time corresponds to the relaxation time of magnetic oscillations and is determined by the dynamics of the magnetization vector when it approaches the equilibrium position.

Possible applications of the effects are discussed. It is demonstrated that the amplitude of the hypersonic elastic oscillations excited in the yttrium-iron garnet in the microwave range amounts to 10^{-9} cm. This level is higher than the levels corresponding to the conventional nonlinear and linear excitations by a factor of greater than 2 and three-to-four orders of magnitude, respectively.

ACKNOWLEDGMENTS

This work was supported by the Russian Foundation for Basic Research (project nos. 12-02-01035-a and 13-02-01401-a).

REFERENCES

1. Y. Kikuchi, *Ultrasonic Transducers* (Corona, Tokyo, 1969; Mir, Moscow, 1972).
2. I. P. Golyamina, "Magnetostriction Radiators from Ferrites," in *Physics and Technology of High-Power Ultrasound,* Vol. 1: *Sources of High-Power Ultrasound*, Ed. by L. D. Rozenberg (Nauka, Moscow, 1967) [in Russian].
3. R. L. Comstock and R. C. LeCraw, J. Appl. Phys. **34**, 3022 (1963).
4. R. C. LeCraw and R. L. Comstock, in *Physical Acoustics. Principles and Methods*, Ed. by W. P. Mason, Vol. 3: *Lattice Dynamics* (Academic, New York, 1964; Mir, Moscow, 1968).
5. H. E. Bommel and K. Dransfeld, Phys. Rev. Lett. **3** (2), 83 (1959).
6. E. G. Spencer, R. T. Denton, and R. P. Chambers, Phys. Rev. **125**, 1950 (1962).
7. F. G. Eggers and W. Strauss, J. Appl. Phys. **34**, 1180 (1963).
8. *Ferrites in Nonlinear Microwave Devices. Collection of Articles*, Ed. by A. G. Gurevich (Inostrannaya Literatura, Moscow, 1961) [in Russian].
9. H. Suhl, J. Phys. Chem. Solids **1** (4), 209 (1957).
10. Ya. A. Monosov, *Nonlinear Ferromagnetic Resonance* (Nauka, Moscow, 1971) [in Russian].
11. V. E. Zakharov, V. S. L'vov, and S. S. Starobinets, Usp. Fiz. Nauk **114**, 609 (1974).
12. Yu. V. Gulyaev, P. E. Zil'berman, A. G. Temiryazev, and M. P. Tikhomirova, J. Commun. Technol. Electron. **44**, 1168 (1999).
13. Yu. V. Gulyaev, P. E. Zil'berman, A. G. Temiryazev, and M. P. Tikhomirova, Phys. Solid State **42**, 1094 (2000).
14. D. I. Sementsov and A. M. Shutyi, Usp. Fiz. Nauk **177**, 831 (2007).
15. V. S. Vlasov, L. N. Kotov, V. G. Shavrov, and V. I. Shcheglov, J. Commun. Technol. Electron. **54**, 821 (2009).
16. F. R. Morgenthaler, IRE Trans. Microwave Theory Tech. **7**, 6 (1959).
17. V. S. Vlasov, L. N. Kotov, V. G. Shavrov, and V. I. Shcheglov, J. Commun. Technol. Electron. **55**, 645 (2010).
18. G. A. Korn and T. M. Korn, *Mathematical Handbook for Scientists and Engineers: Definitions, Theorems, and Formulas for Reference and Review* (McGraw-Hill, New York, 1961; Nauka, Moscow, 1968).
19. A. G. Gurevich and G. A. Melkov, *Magnetic Oscillations and Waves* (Nauka, Moscow, 1994; CRC, Boca Raton, Fl., 1996).
20. S. G. Kalashnikov, *Electricity* (Nauka, Moscow, 1964) [in Russian].
21. D. V. Sivukhin, *General Courses of Physics*, Vol. 3: *Electricity* (Nauka, Moscow, 1977) [in Russian].
22. S. P. Strelkov, *Mechanics* (Nauka, Moscow, 1965) [in Russian].

Translated by A. Chikishev